werden sollen, genügt es bekanntlich nicht[11], die Streuung des Polarons (und hier die des Exzitons) mit der Störungstheorie 1. Ordnung zu berechnen (wie dies etwa in der Leitfähigkeitstheorie der Metalle üblich ist), da wegen der endlichen Anregungsenergie $\hbar\omega$ der optischen Gitterquanten beim Einzelstoß Energie- und Impulssatz nicht gleichzeitig erfüllbar sind. (Ferner macht die starke Kopplung zwischen Gitterschwingungen und Teilchen die Anwendbarkeit der Störungstheorie überhaupt fraglich.) Wir benutzten daher den für die Berechnung der Polaronenbeweglichkeit von Low und PINES[12] entwickelten Formalismus. Die Übertragung auf den vorliegenden Fall bereitet keine Schwierigkeiten und ergibt zunächst für die freie Flugzeit τ des Exzitons

$$\frac{1}{\tau} = e^{-\hbar\omega/kT}\left(\frac{M^*}{M}\right)^2 \frac{2\alpha\omega}{g(\alpha,\mu_i,r_0)}\left\{[1+(r_0 w_0 \mu_2/2)^2]^{-2} - [1+(r_0 w_0 \mu_1/2)^2]^{-2}\right\}^2.$$

Darin ist M die effektive Gesamtmasse des Exzitons im *ruhenden*, M^* die im *schwingenden* Gitter. $g(\alpha,\mu_i,r_0)$ ist gleich 1 für $\alpha=0$ und hängt nur sehr schwach von α ab. w_0 ist näherungsweise durch $(2M\omega/\hbar)^{1/2}$ gegeben. — Die freie Weglänge erhalten wir dann sofort aus der Beziehung $l=v\tau$, wo v die Geschwindigkeit des Exzitons ist.

Bei gleichen scheinbaren Massen von Elektron und Defektelektron wird die freie Weglänge unendlich, da das Exziton für die Polarisationswellen, wie schon MEYER[7] hervorhob, dann als elektrisch neutral erscheint (wenigstens bei den hier betrachteten kleinen Bahnradien). Vor allem in diesem Grenzfall wird es notwendig sein, auch die Streuung des Exzitons an den akustischen Gitterschwingungen zu berücksichtigen, was ohne weiteres (s. z. B. Anm. [10]) mit Hilfe der Störungstheorie 1. Ordnung durchgeführt werden kann.

[12] F. E. Low u. D. PINES, Phys. Rev. **98**, 414 [1955].

Anomaly of Carrier Lifetime in Germanium Bicrystals

By H. F. MATARÉ and B. REED

Research Laboratory, Tung-Sol Electric, Inc.
Bloomfield, New Jersey, USA

(Z. Naturforschg. **11 a**, 876—878 [1956]; eingeg. am 10. September 1956)

Lifetime of minority carriers is known to be strongly structure-sensitive. Especially dislocations in or near the edge orientation may act as recombination centers when the acceptor levels of the dangling bonds are filled.

Recombination at lineage boundaries where the angle of misfit between the grains is about a minute of an arc has been measured already by the ΔX-method (MORTON-HAYNES Method[1]). The change in slope of the potential versus X-Curve indicated a higher recombination rate at the lineage boundary. A very different behavior is found for medium angle grain boundaries where the angle of misfit lies between 1° and 25°. Such bicrystals have been grown in this laboratory using the double seed method and their electrical effects have been described by one of us[2]. The crystals were grown from normal N-type zone purified, antimony-doped germanium (1 to 5 Ohm · cm). Both bicrystal sides showed normal to high lifetime values and a rather perfect structure (etch pit density 10^4 to $10^5\,\mathrm{cm}^{-2}$). A microphotograph of a typical bicrystal surface, preferentially etched, is shown in Fig. 1 * (Bicrystal 20° tilt-angle, twist and rotation zero, 1600×).

A special lifetime measurement set based on the MORTON-HAYNES method allowed taking a lifetime topography of a total crystal surface. The sample could be moved in all dimensions with micrometer drive (1/10 of a mil.). Also, the collector-whisker could be set at any point of the crystal surface. The light is injected from the top such that the observer can see light spot and collector probe and their relative position using a binocular microscope.

The measurements are sub-divided into three major groups:

A) Measurements with light line source on the monocrystal sides (line width 4 mils).

B) Measurements with a light line source moving perpendicularly across the grain-boundary interface.

C) Measurements with a point light source (diameter $\phi = 10$ mils) moving perpendicularly and parallel to and in the grain-boundary line.

In addition, the influences of collector forming and collector-bias as well as grain-boundary to collector spacing were studied.

Fig. 2 shows typical results of such measurements. As is to be expected, the light intensity has a strong effect on the actual value of τ since a considerable number of shallow traps can be filled and the apparent lifetime increased by either background illumination or higher intensity of the migrating light beam. (See upper curve in Fig. 2 which shows same change in slope at the grain-boundary as found by VOGEL, READ, et al.[1]). Details of the structural influence on τ are brought out, however, with a moderate light intensity. The lower curve in Fig. 2 shows a new effect which is an *increase* in the number of holes collected when the light beam crosses the grain-boundary region.

The grain-boundary tilt angle in this case is $25° \pm 1/4°$. The twist and rotational angles are $0° \pm 1/4°$.

Fig. 3 shows the result for a grain-boundary with a 20° tilt angle, where the effect is more striking. The maximum at the grain-boundary was also measured

[1] F. L. VOGEL, W. T. READ, and L. C. LOVELL, Phys. Rev. **94**, 1791 [1954].

[2] H. F. MATARÉ, Phys. Rev. **98**, 1179 [1955]. — Z. Naturforschg. **10 a**, 640 [1955]. — Z. Phys. **145**, 206 [1956].

* Fig. 1 on p. 878 a.

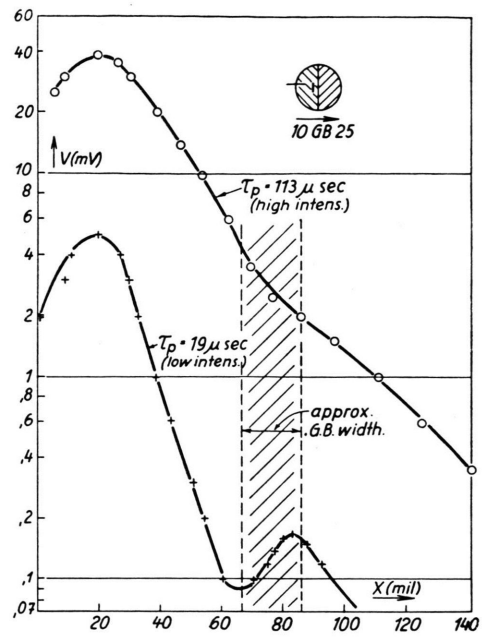

Fig. 2. Typical potential readings versus ΔX (lifetime) across a Ge grain-boundary (G.B.) ($\Theta = 25°$).

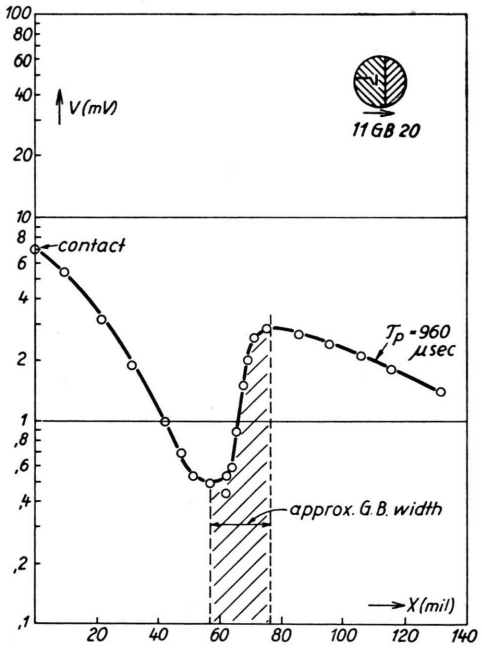

Fig. 3. Typical potential readings versus ΔX across a Ge grain-boundary ($\Theta = 20°$).

for various distances of the collector from the grain-boundary and for various collector potentials. A higher collector voltage as well as a collector approaching the grain-boundary may exert its influence into the grain-boundary zone and thus cover this effect.

(A more detailed description and results will be given in a forthcoming analysis in this Journal.)

Due to the relatively large width of the electrical disturbance at the grain-boundary interface (up to 20 mils), an explanation can be given based on the field of the dangling bonds and the elastic deformation of the lattice in the grain-boundary region. The alternating dilation and compression zones create an alternating width of the forbidden gap while the dangling bonds introduce extra energy levels in the gap. The capture cross-section for incident photons will be higher since these defect-acceptor-levels present typical SCHOTTKY-type recharging centers near the middle of the gap [3]. In addition, the lattice can match different amounts of phonon-energy set free in the hole – electron pair generation.

The slope of the lower curve in Fig. 2 or of the curve in Fig. 3 suggests, however, that here the grain-boundary acts strongly on the drifting holes long before the light spot reaches the grain-boundary zone. The maximum of ΔV at the grain-boundary interface is partially caused by the filling of free bonds (surface states) at the grain-boundary layer which then no longer acts as a sink. In addition, the high capture cross-section or hook action may cause an increased pair release and thus more holes are drifting towards the collector when the light spot crosses the grain-boundary layer. The filling of the free bonds with electrons during strong injection suggests also a build up of a strong SCHOTTKY-type blocking layer at both grain-boundary interfaces [2].

Another striking property of such grain-boundary zones is the very long lifetime measured along such interfaces. A light spot method is used here to reveal a situation as given in Fig. 4. When collector and light spot (diameter 10 mils) are both in the grain-boundary layer, τ reaches high values as compared to the values measured at both monocrystal sides of the bicrystal.

This can be understood if one assumes:

1. That the grain-boundary of a bicrystal grown with considerable precision represents a new "perfect" lattice structure with a constant distance $D = A/2 \sin \Theta$ (A = lattice constant, Θ = angle of misfit between the two grains) between the edge dislocations (low scattering).

2. That holes can easily change position between adjacent bonds in a grain-boundary layer with overlapping wave functions when the dangling bonds are charged up with electrons liberated by photon injection.

The light-point method used here is more appropriate and yields a further localizing behavior. The solution for the diffusion equation for this case:

$$\nabla p^2 = \frac{p}{L_p^2} \tag{1}$$

with

$$L_p^2 = D\,\tau \tag{2}$$

[3] W. SCHOTTKY, Halbleiter-Probleme I, Vieweg, 1954, p. 85 ff.

using a point source, is:

$$P(r) = -\left(\frac{i\,r}{L_p}\right)^{-1/2} p_0\, H_{1/2}^{(1)}\left(\frac{i\,r}{L_p}\right) \qquad (3)$$

with:

$H_{1/2}^{(1)}\left(\frac{i\,r}{L_p}\right)$ = HANKEL Function of order 1/2 and of first kind,

p = excess minority carrier density,

L_p = diffusion length, $\quad i = \sqrt{-1}$,

D = diffusion constant, $\quad r$ = distance collector light,

τ = lifetime, $\quad p_0$ = source excess density.

(3) is equivalent to[4]:

$$p(r) = \sqrt{\frac{2}{\pi}}\,\frac{e^{-r/L_p}}{r/L_p}\cdot p_0\,. \qquad (4)$$

Using the boundary conditions:

$$\left.\begin{aligned} p(r_0) &= \sqrt{\frac{2}{\pi}}\; p_0\;\frac{e^{-r_0/L_p}}{r_0/L_p} \\ p(\infty) &= 0 \end{aligned}\right\} \qquad (5)$$

the partial logarithm of (4) is:

$$\frac{\partial \ln p}{\partial r} = -\left[\frac{1}{L_p} + \frac{1}{r}\right]. \qquad (6)$$

Since the voltage at the probe at distance r from the light is proportional to p it follows:

$$\frac{\partial \ln V}{\partial r} = -\left[\frac{1}{L_p} + \frac{1}{r}\right]. \qquad (7)$$

The light spot diameter has to fulfill the condition $\phi < r$.

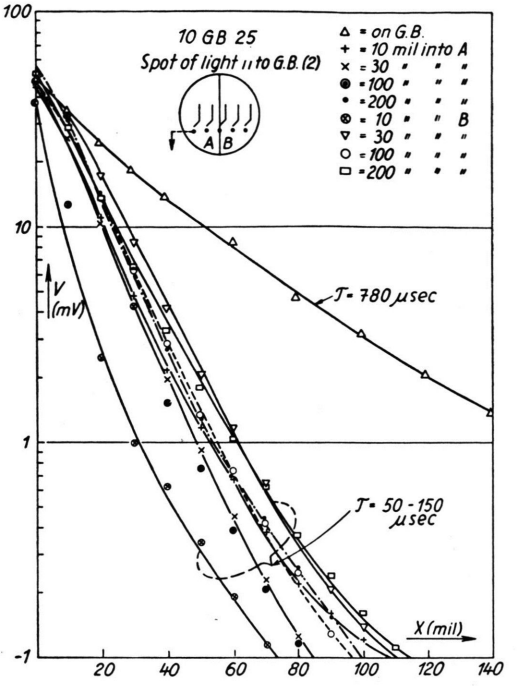

Fig. 4. Results of lifetime measurements parallel to the grain-boundary-interface. τ-maximum in grain-boundary zone.

The authors acknowledge thankfully the co-operation of O. WEINREICH, R. WEGENER, and B. LEVINGER of this laboratory in the construction of special equipment, X-ray seed orientation and bicrystal growth.

It is a pleasure to thank W. T. READ, Jr. for interesting discussions.

[4] See, e. g. JAHNKE–EMDE, 3rd Edition, p. 136 [1938].

Temperatur und Präparatveränderungen im Elektronenmikroskop

Von KARL-JOSEPH HANSZEN

Mitteilung aus der Physikalisch-Technischen Bundesanstalt, Braunschweig

(Z. Naturforschg. **11 a**, 878—880 [1956]; eingegangen am 24. August 1956)

In zahlreichen Untersuchungen[1] wurden an elektronenmikroskopischen Präparaten unter der Elektronenbestrahlung Veränderungen des Kristallgefüges, des Aggregatzustandes und der chemischen Zusammensetzung festgestellt. Eine Reihe dieser Umwandlungen ist offensichtlich auf die im Elektronenstrahl auftretende Objekterwärmung[2] zurückzuführen. Es darf aber nicht außer Acht gelassen werden, daß die pauschale Temperaturerhöhung der Präparate im Elektronenstrahl nur eine Folge der diskreten Wechselwirkung der einfallenden Elektronen mit den getroffenen Molekeln ist, die sich selbst in Anregung, Ionisation und anderen molekularen Veränderungen äußert, also in solchen Erscheinungen, die bei einer Erwärmung des Präparats im Ofen auf die sich im Elektronenmikroskop einstellende Temperatur nicht auftreten. Darüber hinaus können auch durch die benutzten Trägerfolien und durch die unter dem Elektronenstrahl sich auf den Objekten ablagernden Kohlebedeckungen[3] andersartige

[1] S. z. B.: E. F. BURTON, R. S. SENNETT u. S. G. ELLIS, Nature, Lond. **160**, 565 [1947]; E. F. WATSON, J. Appl. Phys. **19**, 713 [1948]; H. KÖNIG, Z. Phys. **130**, 483 [1951]; R. B. FISCHER, J. Appl. Phys. **25**, 894 [1954]; E.W. FISCHER u. H. RICHTER, Ann. Phys. (6) **16**, 193 [1955]; weitere Arbeiten l. c. [4, 5, 6, 8, 10].

[2] Rechnungen hierüber insbes. von B. v. BORRIES u. W. GLASER, Kolloid Z. **106**, 123 [1944].

[3] H. KÖNIG, Z. Phys. **129**, 491 [1951].